

Magnetic Field Observations of Star Formation Regions

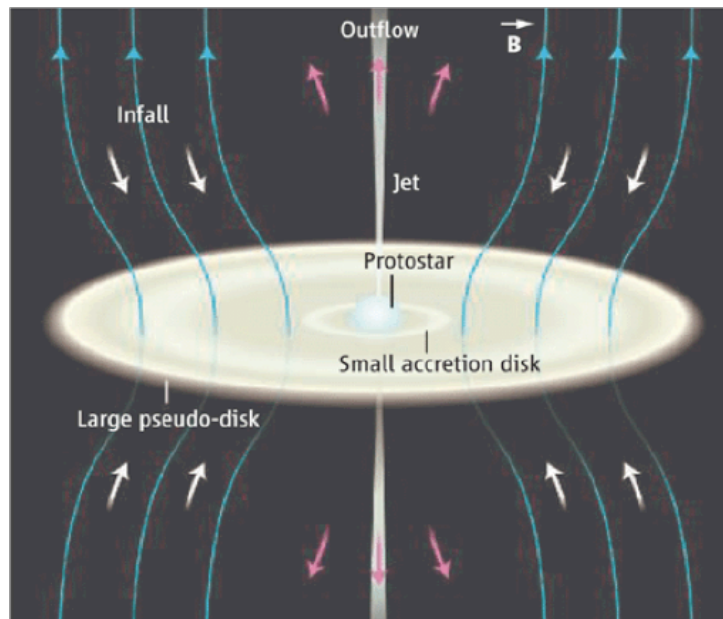
Richard M. Crutcher
University of Illinois



Star formation theory – two extreme cases

1. Strong magnetic fields

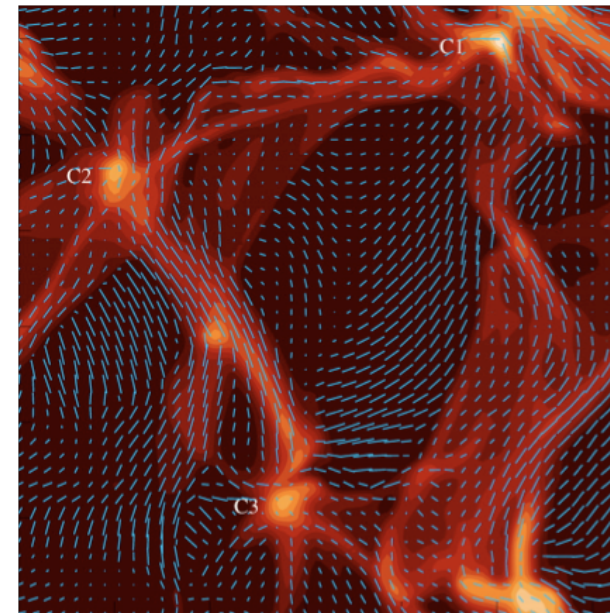
Clouds are magnetically supported, but neutrals contract through the ions that remain frozen to the magnetic field (ambipolar diffusion). When the core mass becomes sufficiently large, core collapse occurs.



Cartoon of star formation with flow down an hourglass morphology magnetic field (Crutcher, Science 313, 771, 2006)

2. Weak magnetic fields

Turbulence leads to formation of clumps, many of which are not self gravitating and dissipate. Those that are dense enough to be self-gravitating are not supported by magnetic pressure and can collapse.



Turbulent simulation of core formation; line segments show the magnetic field (Padoan et al., ApJ 559, 1005, 2001)

Observational Techniques

1. Zeeman effect

- Stokes V spectra yield line-of-sight magnetic field strength, $B(\text{los})$
- mapping can yield maps of line-of-sight magnetic field strengths
- only H I, OH, and CN Zeeman have been detected in the non-masing ISM; however these cover $10 \text{ cm}^{-3} < n(\text{H}) < 10^6 \text{ cm}^{-3}$, wide enough to study star formation processes
- statistical studies are necessary to infer mean or median total field strengths in a sample of clouds, and/or to infer the PDF of the full field strength for a sample of clouds

2. Goldreich-Kylafis effect

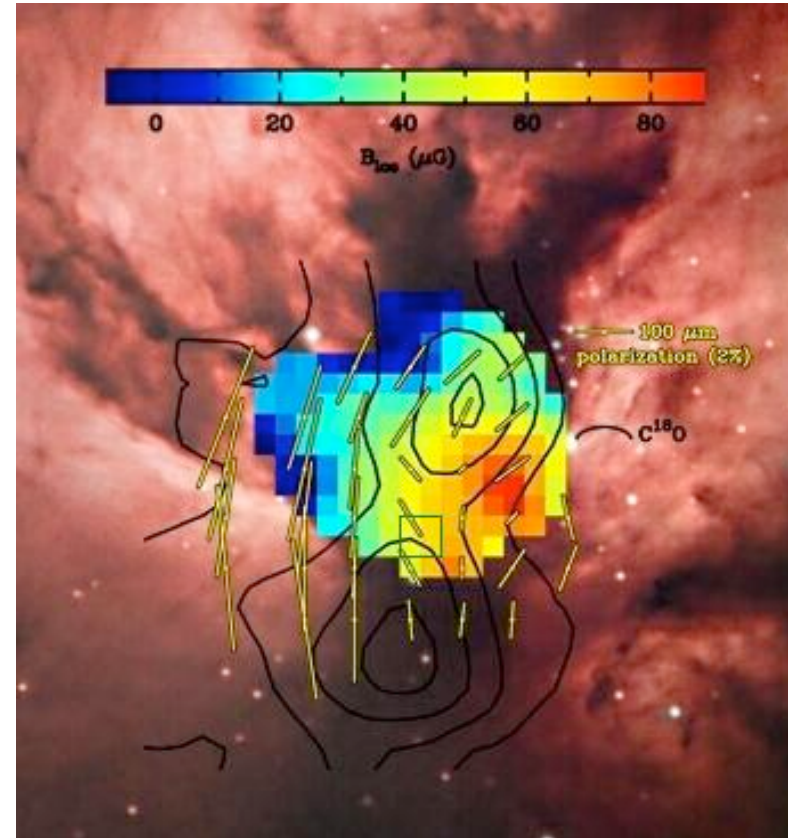
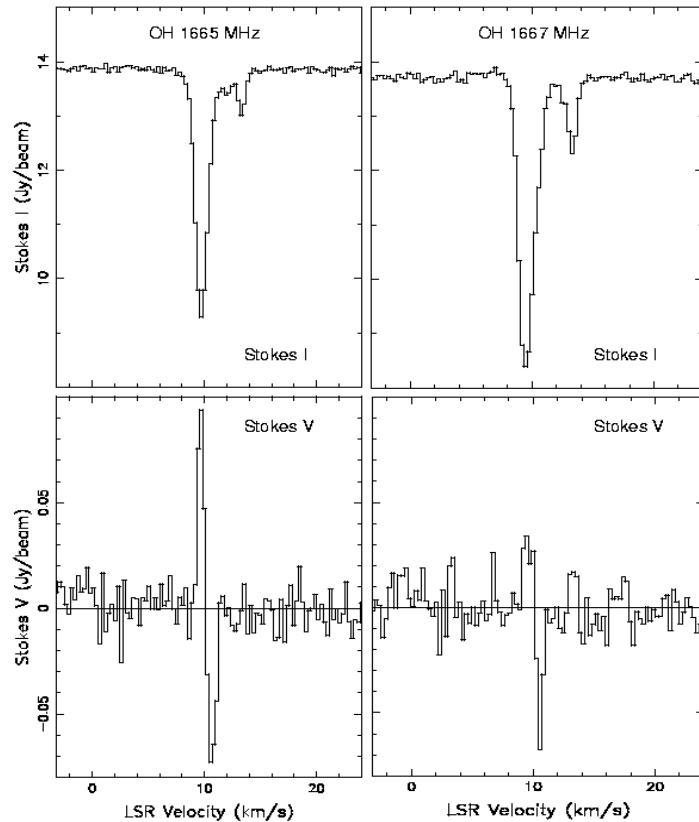
- Stokes Q and U spectra of e.g. CO yield direction of plane-of-sky magnetic field, $B(\text{pos})$
- possible for any molecular line; requires radiative dominating collisional excitation and line optical depth ~ 1 , so different physical conditions may be sampled by different lines

3. Dust polarization

- Stokes Q and U continuum from dust emission yield direction of plane-of-sky magnetic field
- samples dominant emission region with coherent field direction along line of sight

For techniques 2 & 3, Chandrasekhar-Fermi method relates dispersion of field direction within a region to mean plane-of-sky field strength over the region.

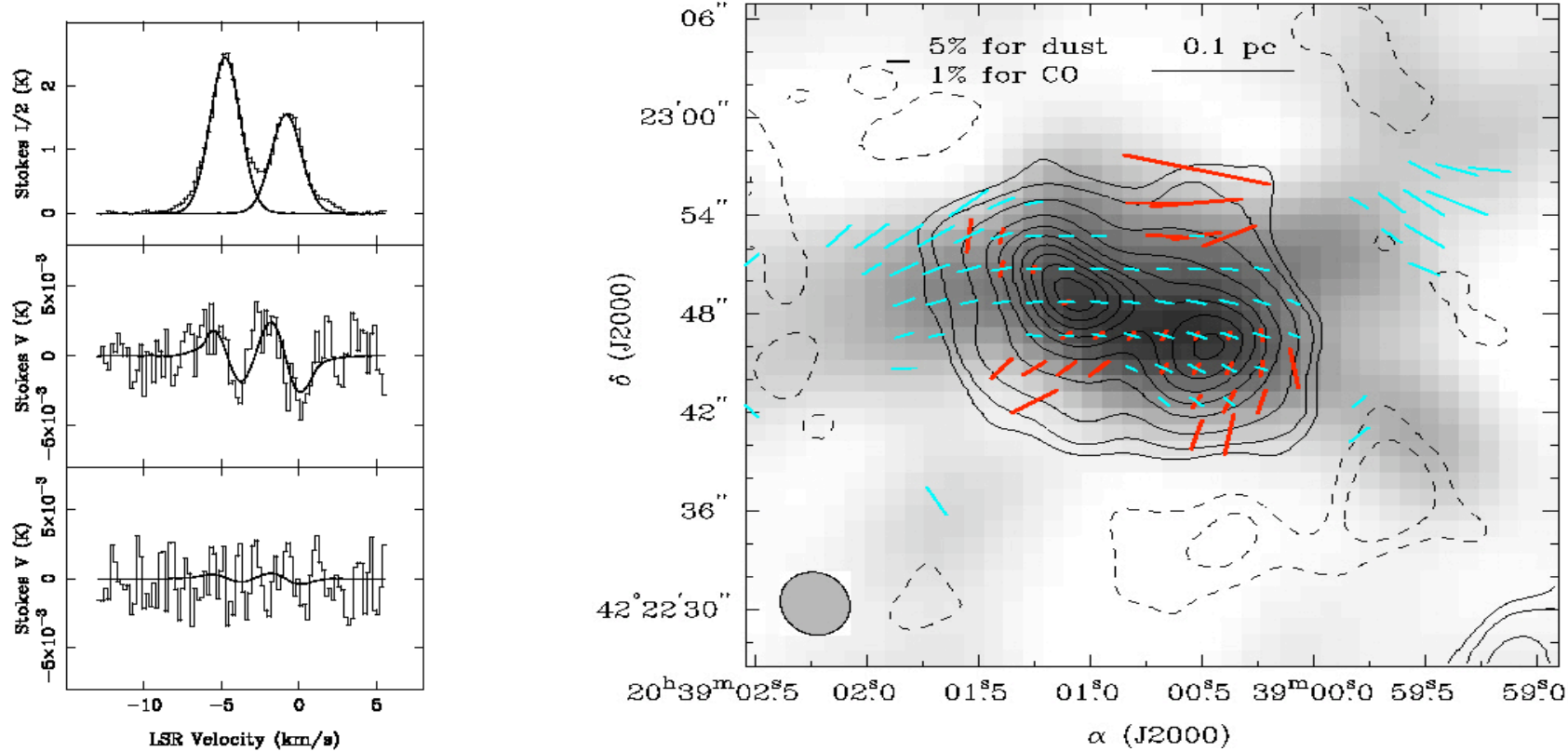
Observational results for NGC2024



Left: VLA OH Zeeman Stokes I and V profiles toward NGC2024 (Crutcher et al. 1999, ApJ 515, 275); $B_{los} \approx 90 \mu\text{G}$.

Right: Optical image of NGC2024 with superposed VLA maps of line-of-sight B_{los} , C^{18}O , and 100 μm dust polarization (Hildebrand et al. 1995, ASP Conf. Ser. 73, 97); $B_{pos} \perp$ the yellow line segments. The field appears to wrap around the NS column of dense gas and dust.

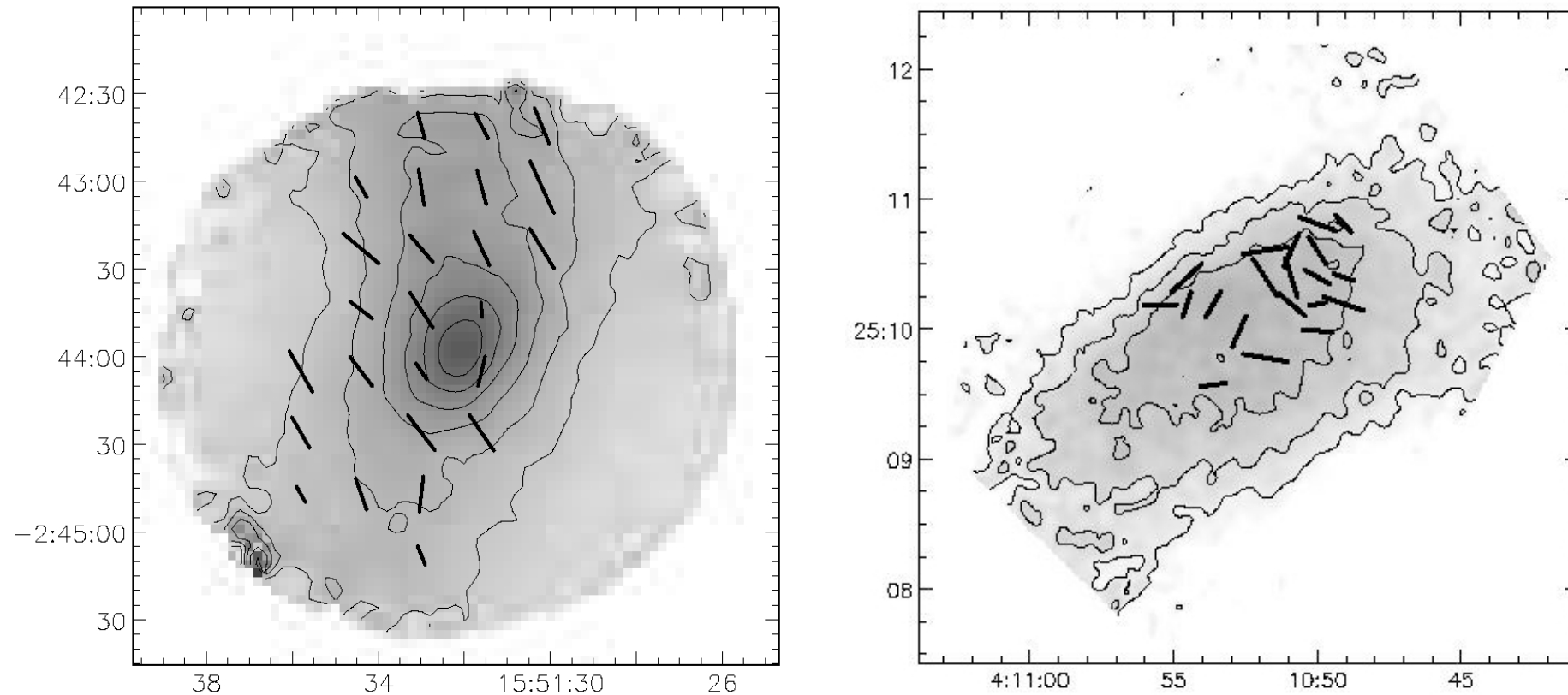
Observational results for DR21OH



Left: CN Zeeman results (Crutcher et al. 1999, ApJ 514, 121). Top panel shows Stokes I average for the 7 hyperfine components, middle panel shows Stokes V average of the four components with strong Zeeman splitting coefficient, bottom panel shows the Stokes V average of the three Stokes V components with very weak Zeeman splitting coefficient. $B(\text{los}) \approx 0.4 \text{ mG} \ \& \ 0.7 \text{ mG}$ for the two velocity components.

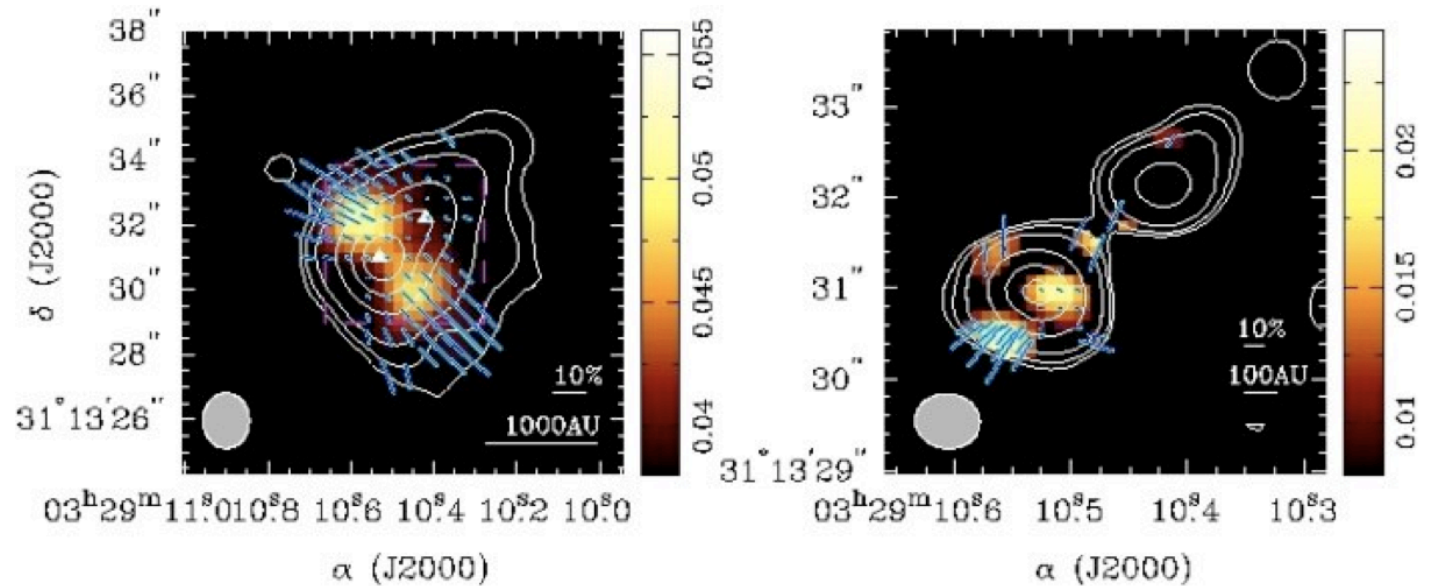
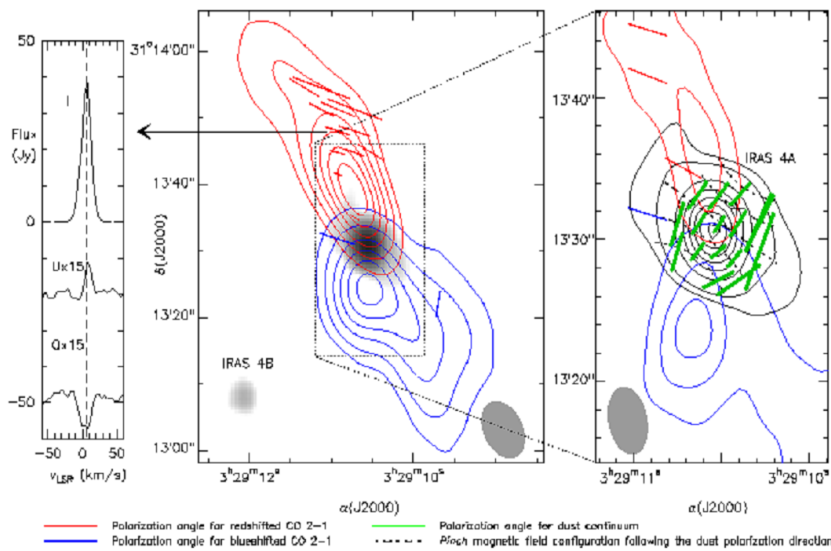
Right: Dust (contours) and CO 2-1 (gray) emission, dust polarization (blue) and CO 2-1 polarization (red). $B(\text{pos})$ is approximately NS, with CO polarization \perp dust polarization. (Lai, Girart & Crutcher 2004, ApJ 598, 392)

Dust polarization maps of starless cores



SCUBA 850 μm maps of L183 (left) and L1498 (right) continuum and magnetic field morphology from dust polarization. Line segments are parallel to $B(\text{pos})$. In L183 the field is well ordered, suggesting that it dominates turbulence, while in L1498 it is fairly random, suggesting turbulence dominates. Even for L183 the field is not along the minor axis, as predicted by idealized strong field, ambipolar diffusion theory (Crutcher et al. 2004, ApJ 600, 279; Kirk et al. 2006, MNRAS 369, 1445).

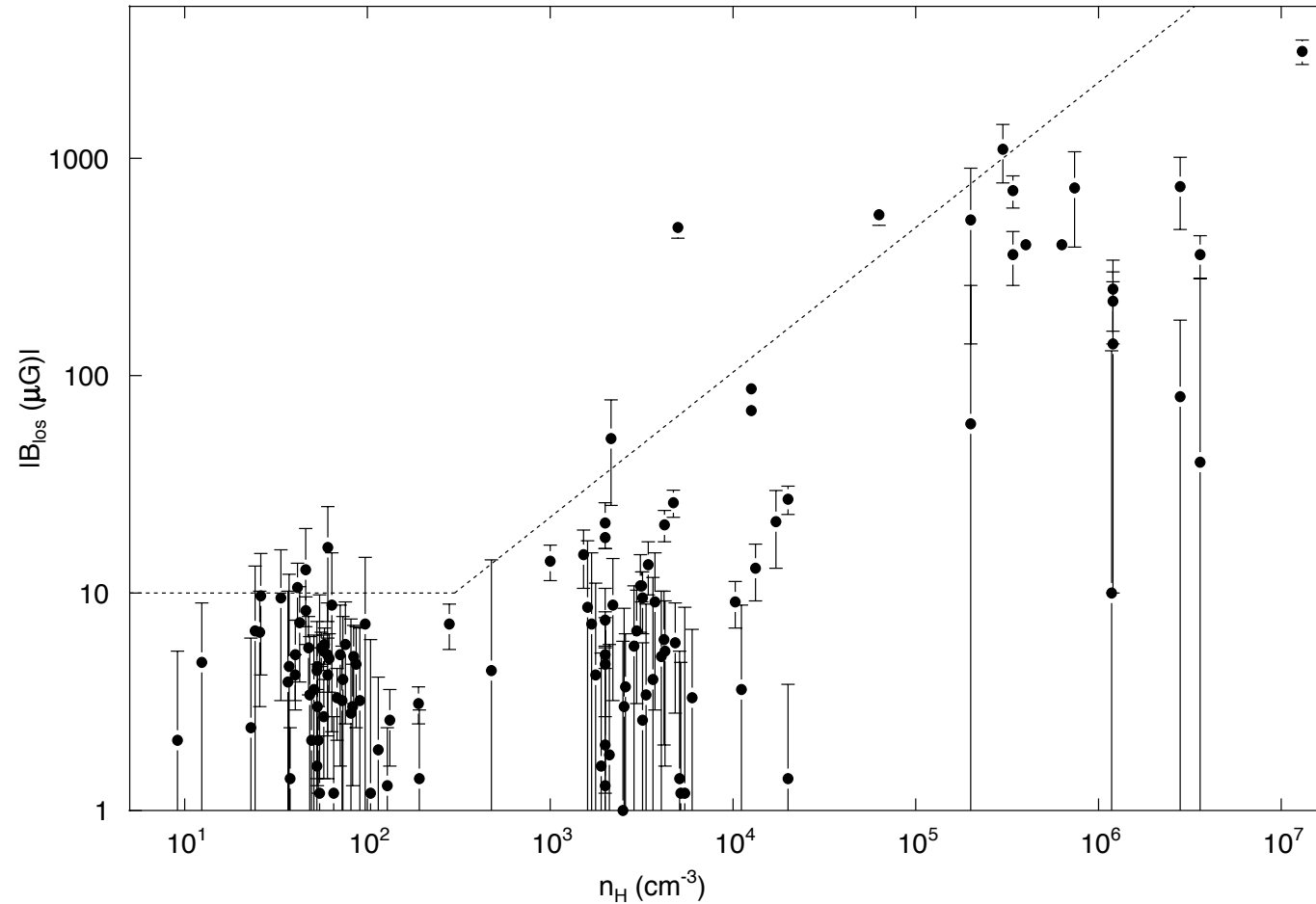
Dust and spectral-line linear polarization results for NGC1333IRAS4



Left: Linear polarization Goldreich-Kylafis effect CO spectral-line and dust continuum maps with BIMA of magnetic field morphology toward the protostar NGC1333IRAS4. The CO map shows the bipolar outflow with the red and blue line segments showing the direction of the magnetic field in the outflow. The green line segments show the dust polarization; the magnetic field is perpendicular to these green line segments. An hourglass morphology field (dotted lines) is suggested. (Girart, Crutcher & Rao 1999, ApJ 525, 109)

Right: SMA maps of dust polarization. The blue line segments show the direction of the magnetic field. At medium spatial resolution (left of the two SMA maps) the field is approximately perpendicular to the pseudodisk with an hourglass morphology, in agreement with the BIMA result. At the highest spatial resolution (rightmost map) with medium and large scale structure resolved out by the interferometer, the field is along the major axis. Modeling supports the picture of an hourglass field along the minor axis at medium spatial scales with a toroidal field in the pseudodisk. (Girart, Rao & Marrone 2006, Science 313, 812; Lai 2010, private communication)

Bayesian analysis of Zeeman results



Results for B_{los} from H I, OH, and CN Zeeman surveys. Bayesian analysis to infer the PDF of the total magnetic field strength B_{tot} from the observed PDF of the line-of-sight component B_{los} yielded $B \propto n^{2/3}$ for $n > 300 \text{ cm}^{-3}$ and $\text{PDF}(B_{\text{total}})$ flat, that is, very weak magnetic fields are as possible as fields up to the dotted line shown on the above figure. These results favor the turbulent, generally weak-field models. (Crutcher et al. 2010, ApJ submitted)

Differential mass-to-flux ratio

The strong field, ambipolar diffusion driven model of star formation requires that the ratio of mass to magnetic flux (M/Φ) *increase* from the envelope to the core region of clouds. Because the Zeeman effect yields only the line-of-sight field strength, and the Chandrasekhar-Fermi method of estimating field strengths from linear polarization data gives only an approximate value of the mean field strength over a region, it is not possible to measure M/Φ for individual positions to test this prediction. However, it is possible to measure the *ratio* of M/Φ between envelope and core, since the unknown angle between the magnetic field and the line of sight will cancel in the ratio. Results for four dark cloud cores (Crutcher et al. 2009, ApJ 692, 844; Crutcher et al. 2010, MNRAS 402, L64) are the following:

<u>Cloud:</u>	<u>L1448</u>	<u>B217-2</u>	<u>L1544</u>	<u>B1</u>
$\frac{M/\Phi(\text{core})}{M/\Phi(\text{envelope})}$	0.21 ± 0.30	0.19 ± 0.46	0.89 ± 0.59	0.37 ± 0.18

Because the ambipolar diffusion model predicts this ratio to be the inverse of the amount by which the cloud was originally subcritical, or >1 , these results do not support this model.

SOFIA mapping of dust polarization in star formation regions

The current state of observational testing of the role of magnetic fields in star formation is that results favor turbulence playing a major and perhaps dominant role, but magnetic fields are sometimes strong enough for magnetic support and ambipolar diffusion to be important. A sensitive polarimeter on SOFIA can address the following questions and help significantly in understanding the fundamental astrophysical problem of how stars form:

1. Giant Molecular Clouds (GMCs)

- Is M/Φ in GMCs supercritical or subcritical?

2. Cores

- Are fields tangled as in L1498 or regular as in L183?
- Are fields aligned with minor axes of putative pseudo-disk structures?
- Do core hourglass morphology fields connect smoothly with larger-scale fields to form a coherent structure, or are cores the intersections of filaments aligned with fields?
- Is there evidence for magnetic braking?

3. Bipolar outflows

- What is the relationship between outflows, thought to be driven by magnetic fields, and field morphology?